Developing a Novel Biomimetic Soft-Actuated Humanoid Endoskeleton for Elderly Assistance

Thesis

Nichelle Thinagar

Massachusetts Academy of Math and Science

85 Prescott St., Worcester, MA

Abstract

More than 70% of people age 65 and older will require long-term care, with 90% of this long-term care being provided by unpaid family and friends. 45% of these caregivers are 55 or older themselves, and one third of all caregivers' health is at or below 2 on a 5-point scale. Thus, robotic options for elder care are vital, often coming in the form of humanoid robots. However, existing humanoid robots are designed for 3D (dirty, dangerous, and demanding) tasks as opposed to human-robot interaction (HRI), making them unsuitable for elder care. Existing rigid humanoid robots (RHRs) cost upward of 16,000 USD, much of this cost coming from expensive high-torque motors and mechanisms and intensive processors. Current RHRs are not morphologically suited to HRI due to the inherent rigidity of their links, which pose a significant injury risk upon collision in a care-oriented environment. Existing soft humanoid robots (SHRs), though, lack the movement capabilities and manipulation stress of RHRs. Furthermore, the pneumatic components used in SHRs are bulky, loud, and heavy, impacting their overall HRI capabilities. Additionally, existing SHR designs are not biomimetic, as they do not take advantage of biological human musculature. Therefore, this work set out to develop a novel, biomimetic, soft-actuated humanoid developed specifically for human interaction. This work focused specifically on the actuation of a lightweight endoskeleton using modified McKibben pneumatic actuators in conjunction with a novel skeleton-integrated low-noise air system. This system uses optimized McKibben actuators, which achieved a ~50% reduction in the pressure necessary for maximum strain after a repeated strain-based stretching and lubrication process. These actuators are able to exert a theoretical maximum linear force of 128.05 N, with a 13.00N force exerted to compress air into the actuator to the minimum observed pressure for maximum contraction of 6 psi. This facilitated the development of a biomimetic elbow joint, which was optimized for human-comparable movement, achieving a maximum bending angle of 180°. When integrated with a 21.25cm actuator module, this elbow joint was capable of lifting a 3.30lb load. This work represents a significant step towards enabling inexpensive soft robotic humanoid robots to assist elderly individuals, potentially impacting a group of over 581 million people and their caregivers.

Acknowledgements

Dr. Ava Lakmazaheri provided valuable insight into human-robot interaction and the fundamentals of human-oriented design.

Dr. Kevin Crowthers supervised and advised this research, specifically the related technical writing.

Developing a Novel Soft Actuated Humanoid for Elderly Assistance

Introduction

As the world's number of people over the age of 65 is set to account for 34% of the population by 2050, devices designed to care for these individuals have become vital to the continued comfort and well-being of this older portion of the world (Sinha et. al.). The need for such technology is especially increased in the case of unpaid caretakers. 90% of individuals providing long-term care for elderly citizens are friends or relatives (Bureau of Labor Statistics). In approximately 50% of such situations, these caregivers themselves are elderly, and in over 30% of cases, unpaid caretakers require health assistance themselves (Bureau of Labor Statistics). In order to provide elder care in place of such unpaid caretakers and relieve the stress of caring for another individual when in poor health, one clear option is humanoid robots. Oftentimes, the tasks that seniors require assistance with — such as opening medicine containers, standing up from a seated position, or retrieving items — are simple to perform for the human form factor (Syrin Raj, Personal Communication). The human physiology is very well-suited to the grasping, lifting, and manipulation necessitated by assistance via the musculoskeletal system while simultaneously being sufficiently gentle and compliant in these actions in order to ensure the comfort and safety of an assistee when care is provided.

However, existing humanoid robots are incredibly expensive, making them very inaccessible to older citizens who require assistance with daily tasks (Unitree). The Unitree G1, which is largely regarded as the most advanced and inexpensive humanoid robot, costs 16,000 USD in its most basic version, rendering it infeasible for use in elder care (Unitree). A large part of this cost comes from the high price of creating compact yet high-power joints (Kaneko et. al.). These joints primarily use motors to drive rotational motion that somewhat replicates human motion as opposed to replicating the biology of human kinematics (Zhang et. al.). This means these motors and the connected mechanisms must be capable of incredibly high torques as they do not rely on the comparatively efficient linear muscular contraction seen in human motion (Sanan et. al.). Furthermore, existing humanoid robots, for the most part, come in rigid

designs, which are best suited to 3D (dangerous, dirty, demanding) tasks such as construction and manufacturing. Due to the physical capability-centric design approach of all functional humanoid robots, they are incapable of the gentleness that is paramount to success in a care environment. This highlights an overarching issue with humanoid robots; they are not designed for human-robot interaction (HRI). HRI is a constant discussion in the robotics space as it is vital to ensuring that technologies are able to be integrated into spaces designed for and utilized by humans. In terms of humanoid robots, HRI is almost entirely discussed in terms of control methods. Often using reinforcement learning, humanoid robots are trained to hone their HRI capabilities solely through their programmed behaviors. Conversely, the space of assistive technology focuses on morphological specifications to improve human interaction abilities (Wang et. al.). Oftentimes, this is achieved through the use of soft technologies such as the pneumatic bellows-based upper limb orthotic designed by Walsh et. al.. When comparing the studies of assistive technology and humanoid robots, it becomes evident that assistive devices such as orthotics and prosthetics are used very effectively in practice, while any assistive capabilities of humanoid robots remain largely theoretical. The key difference between these technologies is that orthotics and prosthetics are designed with the intention of direct HRI, while HRI is a secondary or tertiary objective of humanoid robots because of their focus on automation tasks — replacing humans rather than working with them. Thus, this study aims to develop a humanoid robot designed with the focus of optimizing it for HRI, thus making it an effective tool for elder care.

A robot's HRI capabilities are defined in three major categories: behavior, morphology, and comfort (Sanan et. al.). Of these categories, humanoid robots are incredibly well-developed in terms of behavioral control. This work focuses primarily on the morphology and comfort of interaction of the robot. In order to optimize the comfort that individuals feel when utilizing the developed device, this study proposes a biomimetic design based on the human musculoskeletal system. Such a design involves three primary components: a lightweight and compact endoskeleton to provide structure to the design while remaining inexpensive and easy to manipulate, compact yet strong "muscles" to articulate that

skeleton, and a soft exoskeleton to ensure gentle external interactions. In using soft actuation for the joints, expensive mechanisms such as harmonic gear-based drive can be eliminated, bringing down overall costs. Eliminating the bulky systems necessary for such mechanisms opens the door for the use of a soft exoskeleton, making the robot better suited to human-robot interaction (HRI). Existing humanoid robots (Figure from Kaneko et al.) listed below are primarily rigid ones used for 3D tasks.

		HRP-5P	HRP-2Kai	TALOS	DRC-Atlas	JAXON	E2-DR
Height [mm]		1,830	1,710	1,750	1,880	1,880	1,680
Weight [kg]		101	65	95	157	127	85
Mean Value of Each Joint	" Joint Power / Weight " *1	1.00	0.50	0.47 *2	1.03	0.74	No Info.
	" Joint Torque / Weight " *1	1.00	0.79	0.48 *2	0.68	1.22	1.01
	Joint Angle Speed *1	1.00	0.65	1.01 *2	1.60	0.62	No Info.
D.O.F. in Total		37 D.O.F.	32 D.O.F.	32 D.O.F.	32 D.O.F.	35 D.O.F.	33 D.O.F.
	Neck	2 D.O.F.	2 D.O.F.	2 D.O.F.	2 D.O.F.	2 D.O.F.	2 D.O.F.
	Arm	2 Arms × 9 D.O.F.	2 Arms × 7 D.O.F.	2 Arms × 7 D.O.F.	2 Arms × 7 D.O.F.	2 Arms × 8 D.O.F.	2 Arms × 8 D.O.F.
	Hand	2 Hands × 1 D.O.F.	2 Hands × 1 D.O.F.	2 Hands × 1 D.O.F.	2 Hands × 1 D.O.F.	2 Hands × 1 D.O.F.	2 Hands × 1 D.O.F.
	Waist	3 D.O.F.	2 D.O.F.	2 D.O.F.	3 D.O.F.	3 D.O.F.	2 D.O.F.
	Leg	2 Legs × 6 D.O.F.	2 Legs × 6 D.O.F.	2 Legs × 6 D.O.F.	2 Legs × 6 D.O.F.	2 Legs × 6 D.O.F.	2 Legs × 6 D.O.F.

*1: Except hand joint *2: Only legs

Though there have been humanoid robots with soft exoskeletons, no effective humanoids use soft actuation. However, by integrating a soft actuation approach into the robot's skeleton, the high cost of joints, their bulkiness, and rigidity in a collision are greatly reduced.

Methodology

This study aims to evaluate the lifting strength (~2.5kg required for domestic applications), actuation strain, actuation stress, actuator stroke, and range of motion of the proposed design through the following procedures using the listed materials.

- (2) kg PLA 3D printer filament
- (1) 3D printer with a minimum build volume of 18cm x 18cm x 10 cm
- (1) Arduino UNO or similar microcontroller
- (1) Breadboard with jumper wires
- (4) 9v batteries
- Jumper wires

- Installation of Arduino IDE
- ⅜” diameter silicon tubing
- Cylindrical craft balloons
- 60 mL syringe
- Oil or similar lubricant
- ½” braided cable sheathing
- Installation of computer-aided design software of choice
- Installation of slicer of choice, such as Ultimaker Cura
- Protractor
- Silicon insert nuts (i.d. 5/16”)

Procedure 1: Range of Motion.

1. Design and fabricate the joint to be tested in the CAD software
2. Create sketch lines defining the central axis of the joint’s two skeletal components
3. Create an assembly simulating the movement of the joint
4. Apply a collision mate to the skeleton components
5. Manipulate the joint to maximum bending angle
6. Measure angle between skeletal midlines

Procedure 2: Strain and Stroke.

1. Fabricate five lengths (5cm, 10cm, 15cm, 20cm, 25cm) of McKibben actuators using silicon tubing, balloons, lock nuts, and cable sheathing
2. Use an electric or hand pump to inflate the 5cm actuator to max contraction
3. Measure the final actuator length and record stroke (initial - final) and strain (final/initial)
4. Repeat 10 times
5. Repeat for all actuator lengths

Statistical Tests

A paired t-test for means was used to determine if the difference in necessary pressure after the stretching and lubrication treatment was statistically significant.

Results

Trial No.	**Initial (Relaxed) Length**	**Contracted Length**	**Stroke Length**	**Strain %**
1	4.85	4.10	0.75	15.46%
2	4.85	4.05	0.80	16.49%
3	4.85	3.90	0.95	19.59%
4	4.85	4.15	0.70	14.43%
5	4.85	3.95	0.90	18.56%
6	4.85	4.00	0.85	17.53%
7	4.85	4.05	0.80	16.49%
8	4.85	4.00	0.85	17.53%
9	4.85	4.15	0.70	14.43%
10	4.85	4.10	0.75	15.46%
Average	**4.85**	**4.05**	**0.81**	**16.60%**
Trial No.	**Initial (Relaxed) Length**	**Contracted Length**	**Stroke Length**	**Strain %**
1	11.80	8.30	3.50	29.66%
2	11.80	8.45	3.35	28.39%
3	11.80	8.95	2.85	24.15%
4	11.80	8.75	3.05	25.85%
5	11.80	8.60	3.20	27.12%
6	11.80	8.45	3.35	28.39%
7	11.80	8.45	3.35	28.39%
8	11.80	8.60	3.20	27.12%
9	11.80	8.95	2.85	24.15%
10	11.80	8.40	3.40	28.81%

Average	**11.80**	**8.59**	**3.21**	**27.20%**
Trial No.	**Initial (Relaxed) Length**	**Contracted Length**	**Stroke Length**	**Strain %**
1	16.15	11.75	4.40	27.24%
2	16.15	11.70	4.45	27.55%
3	16.15	11.80	4.35	26.93%
4	16.15	11.70	4.45	27.55%
5	16.15	11.80	4.35	26.93%
6	16.15	11.65	4.50	27.86%
7	16.15	11.80	4.35	26.93%
8	16.15	11.95	4.20	26.01%
9	16.15	11.75	4.40	27.24%
10	16.15	11.70	4.45	27.55%
Average	**16.15**	**11.76**	**4.39**	**27.18%**
Trial No.	**Initial (Relaxed) Length**	**Contracted Length**	**Stroke Length**	**Strain %**
1	22.85	16.20	6.65	29.10%
2	22.85	16.05	6.80	29.76%
3	22.85	16.15	6.70	29.32%
4	22.85	16.10	6.75	29.54%
5	22.85	16.30	6.55	28.67%
6	22.85	16.25	6.60	28.88%
7	22.85	16.00	6.85	29.98%
8	22.85	16.35	6.50	28.45%
9	22.85	16.45	6.40	28.01%
10	22.85	16.50	6.35	27.79%
Average	**22.85**	**16.24**	**6.62**	**28.95%**
Trial No.	**Initial (Relaxed) Length**	**Contracted Length**	**Stroke Length**	**Strain %**
1	24.50	17.65	6.85	27.96%
2	24.50	17.85	6.65	27.14%
3	24.50	17.80	6.70	27.35%
4	24.50	17.80	6.70	27.35%
5	24.50	17.80	6.70	27.35%
6	24.50	17.60	6.90	28.16%

7	24.50	17.50	7.00	28.57%
8	24.50	17.75	6.75	27.55%
9	24.50	17.70	6.80	27.76%
10	24.50	17.40	7.10	28.98%
Average	**24.50**	**17.69**	**6.82**	**27.82%**

Table 1 contains the actuator strain and stress data.

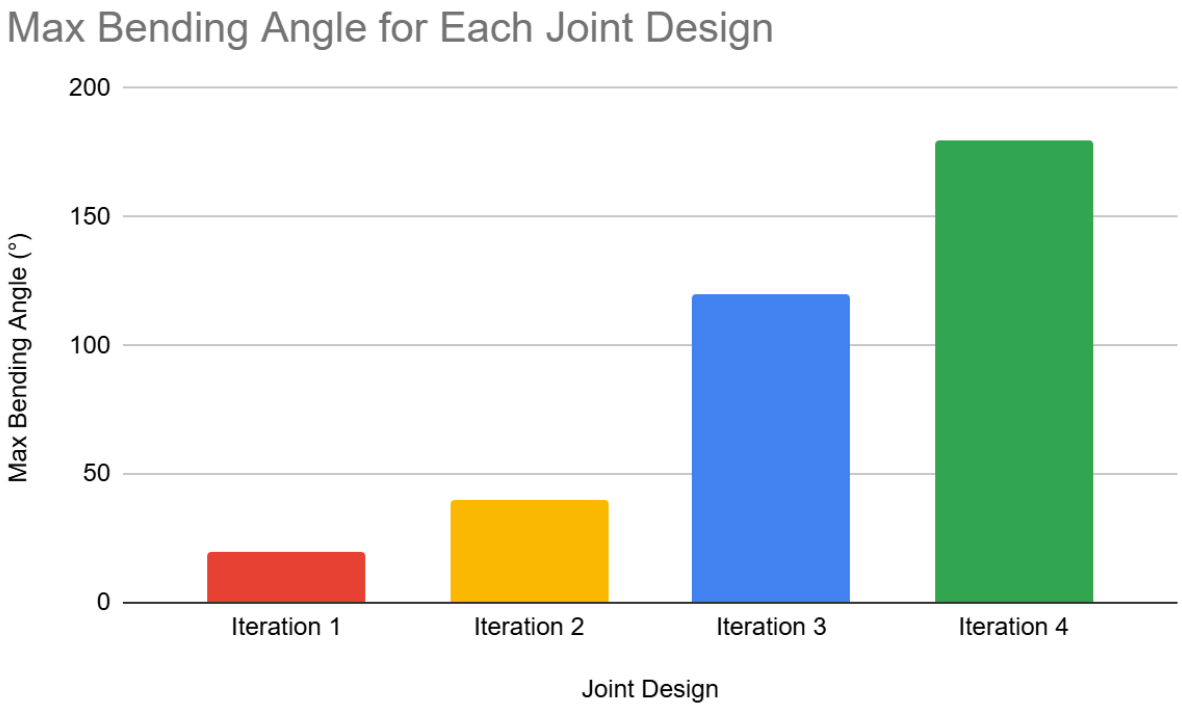

Figure 1 shows the maximum bending angle of each iteration of the elbow joint skeleton.

Trial No.	Acceleration (m/s^2)	dv/dx (m/s^2)	Cart Mass (kg)	Force (N)
1	1.546	1.478	1.7968	2.72
2	1.409	1.346	1.7968	2.48
3	1.524	1.458	1.7968	2.68
4	1.455	1.399	1.7968	2.56

5	1.436	1.216	1.7968	2.38
6	1.397	1.335	1.7968	2.45
7	1.192	1.153	1.7968	2.11
8	1.108	1.059	1.7968	1.95
9	1.165	1.115	1.7968	2.05
10	1.263	1.207	1.7968	2.22
Average	**1.350**	**1.277**	**1.7968**	**2.36**
Trial No.	**Acceleration (m/s^2)**	**dv/dx (m/s^2)**	**Cart Mass (kg)**	**Force (N)**
1	0.117	0.116	1.7968	0.21
2	0.132	0.136	1.7968	0.24
3	0.121	0.125	1.7968	0.22
4	0.070	0.085	1.7968	0.14
5	0.049	0.057	1.7968	0.10
6	0.118	0.130	1.7968	0.22
7	0.221	0.214	1.7968	0.39
8	0.287	0.312	1.7968	0.54
9	0.198	0.194	1.7968	0.35
10	0.200	0.220	1.7968	0.38
Average	**0.151**	**0.159**	**1.7968**	**0.28**
Trial No.	**Acceleration (m/s^2)**	**dv/dx (m/s^2)**	**Cart Mass (kg)**	**Force (N)**
1	0.850	0.821	1.7968	1.50
2	0.860	0.946	1.7968	1.62
3	0.896	0.790	1.7968	1.51
4	0.970	0.941	1.7968	1.72
5	0.785	0.755	1.7968	1.38
6	0.826	0.799	1.7968	1.46
7	0.841	0.803	1.7968	1.48
8	0.796	0.818	1.7968	1.45
9	0.748	0.718	1.7968	1.32
10	0.704	0.685	1.7968	1.25
Average	**0.828**	**0.808**	**1.7968**	**1.47**
Trial No.	**Acceleration (m/s^2)**	**dv/dx (m/s^2)**	**Cart Mass (kg)**	**Force (N)**
1	1.492	1.333	1.7968	2.54
2	1.349	1.310	1.7968	2.39

3	1.168	1.268	1.7968	2.19
4	1.388	1.490	1.7968	2.59
5	1.287	1.369	1.7968	2.39
6	1.295	1.466	1.7968	2.48
7	1.384	1.581	1.7968	2.66
8	1.466	1.422	1.7968	2.59
9	1.223	1.121	1.7968	2.11
10	1.187	1.074	1.7968	2.03
Average	**1.324**	**1.343**	**1.7968**	**2.40**
Trial No.	**Acceleration (m/s^2)**	**dv/dx (m/s^2)**	**Cart Mass (kg)**	**Force (N)**
1	1.456	1.413	1.7968	2.58
2	1.451	1.395	1.7968	2.44
3	1.535	1.523	1.7968	2.75
4	1.431	1.363	1.7968	2.51
5	1.458	1.572	1.7968	2.72
6	1.132	1.219	1.7968	2.11
7	1.452	1.406	1.7968	2.57
8	1.628	1.563	1.7968	2.87
9	1.222	1.190	1.7968	2.17
10	1.458	1.261	1.7968	2.44
Average	**1.422**	**1.391**	**1.7968**	**2.51**

Table 2 shows the instantaneous force each actuator is capable of producing.

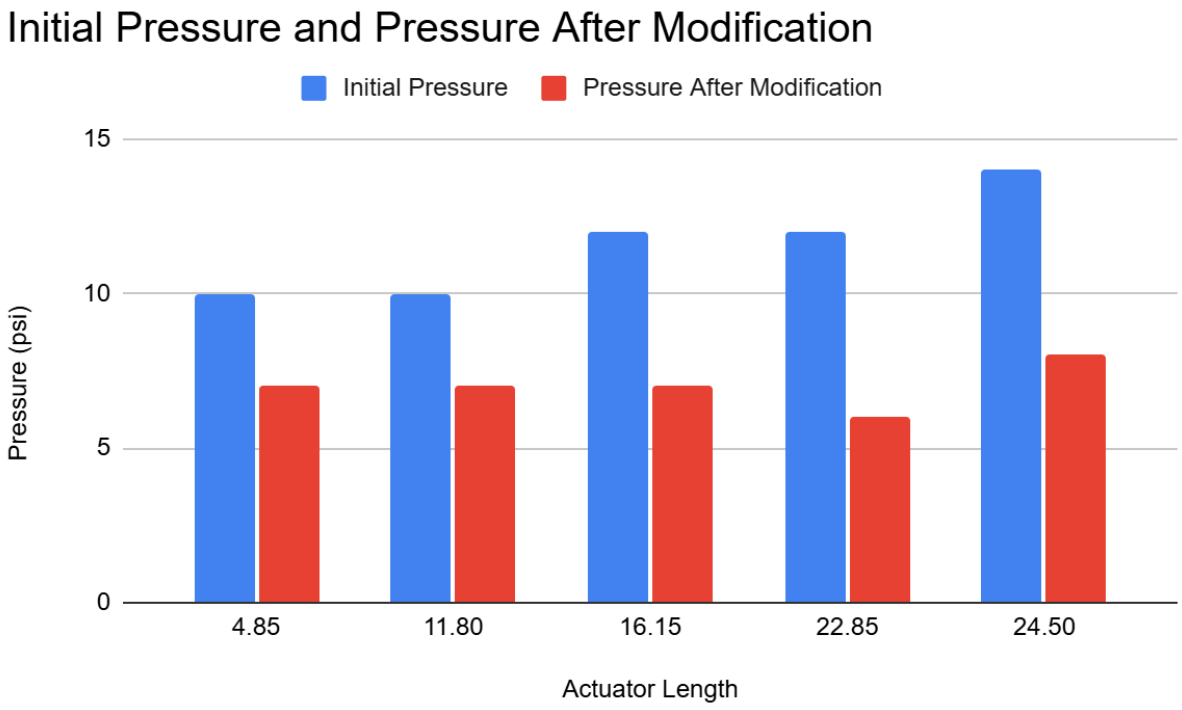

Figure 2 shows the change in pressure after the lubrication and stretching treatment.

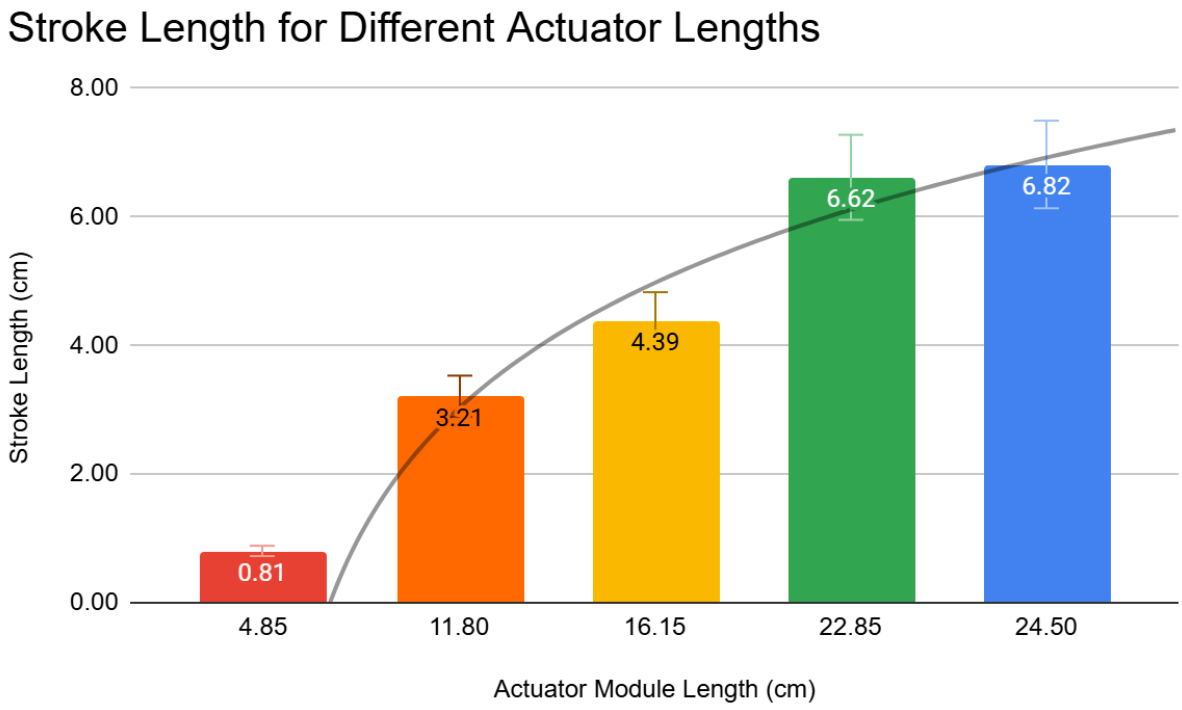

Figure 3 shows the trend in actuator stroke length over different actuator lengths. The correlation coefficient calculated for this trend is 0.9979.

$$F = P \cdot A$$

Where P is the required pressure (min. 6 psi) and A is the cross-sectional area of the cylinder ($\pi \cdot r^2$: $r = 0.01m$)

$$F = 41368.5_{(pascals)} \cdot \pi \cdot 0.0001 = 13.00\text{N}$$

This indicates that 13 Newtons of linear force are required to inflate the actuator to maximum contraction

$$F = P\pi r_0^2(3cot^2(\theta_0)(1 - k(1 - \frac{h}{h_0})) - csc^2(\theta_0))$$

This equation describes the force exerted by a McKibben Actuator inflated with gauge pressure P, an initial outer braid angle of θ_0 (18.30°), radius of r_0 (1.35cm), initial and final length of h_0 and h (21.25cm and 16.00cm), respectively, and a fudge factor k (generally 1.30) to account fokkr possible friction during contraction

$$F = 128.05\text{N}$$

Due to the friction-reducing measures implemented, k is assumed to be 1.00, and P is defined as the minimum observed pressure for maximum contraction (6 psi)

Figure 4 displays the mathematical calculations for the force input to and output from the 21.25cm actuator module.

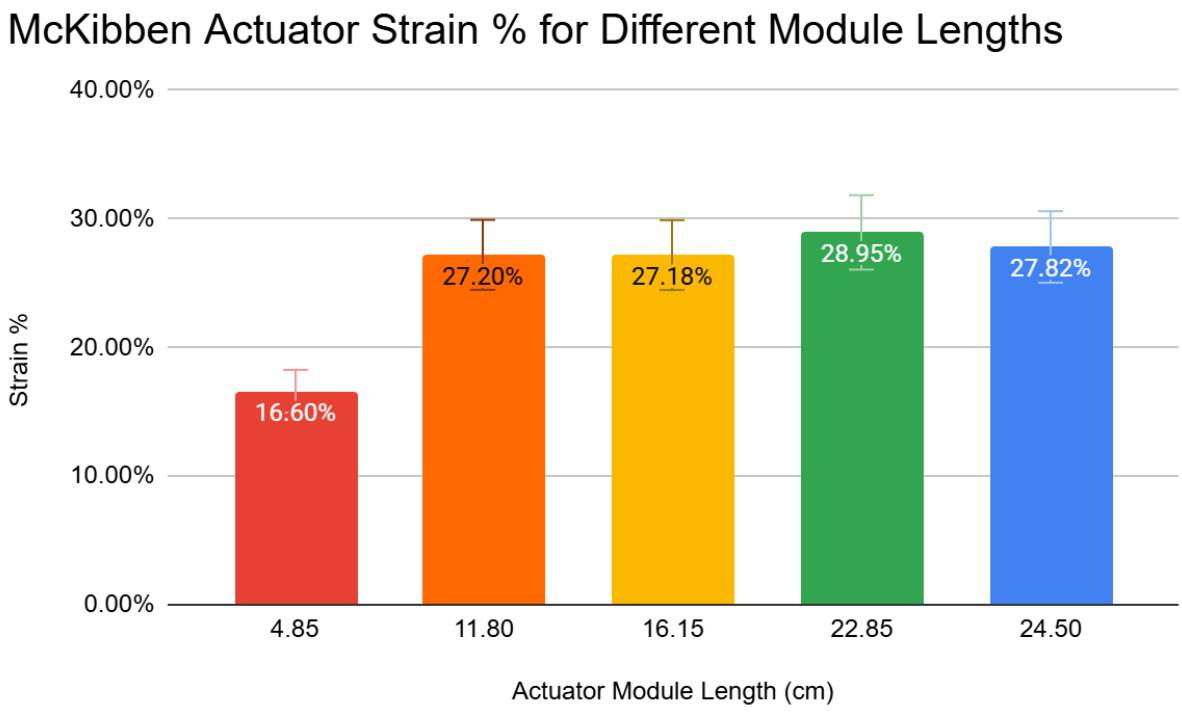

Discussion

These results indicated which actuator lengths are capable of the maximum contraction percentage (strain). The 22.85cm and 24.50cm modules performed the best with actuation strains of 28.95% and 27.82%, respectively. The 24.50cm module was selected for the prototype due to its superior stroke (contraction distance) of 6.82cm. Actuators showed a logarithmic trend in stroke (the distance contracted) where: Stroke = -5.46 + 3.74 ln(Actuator Length) with r = 0.9799 and R2 = 96.02%. This indicates that the optimal actuator length is between ~22.50cm and 30cm. This led to the selection of 24.05cm module for best stroke and length within optimal range.

Future Research

Going forward, this research will integrate compact high torque gearing into skeletal cavities, implement noise-damping materials into motor housing, integrate a soft pneumatic upper limb end effector, and implement camera-based object detection. This research will then develop an IK-based control system with a ROS-2 hardware interface and Raspberry-pi. This work will then fabricate and integrate a soft exoskeleton for the upper body endoskeleton and train the device to perform everyday tasks using existing software.

Section V: Conclusion

This research developed a novel compact airflow system for a soft humanoid robot and a novel joint design (see figures below).

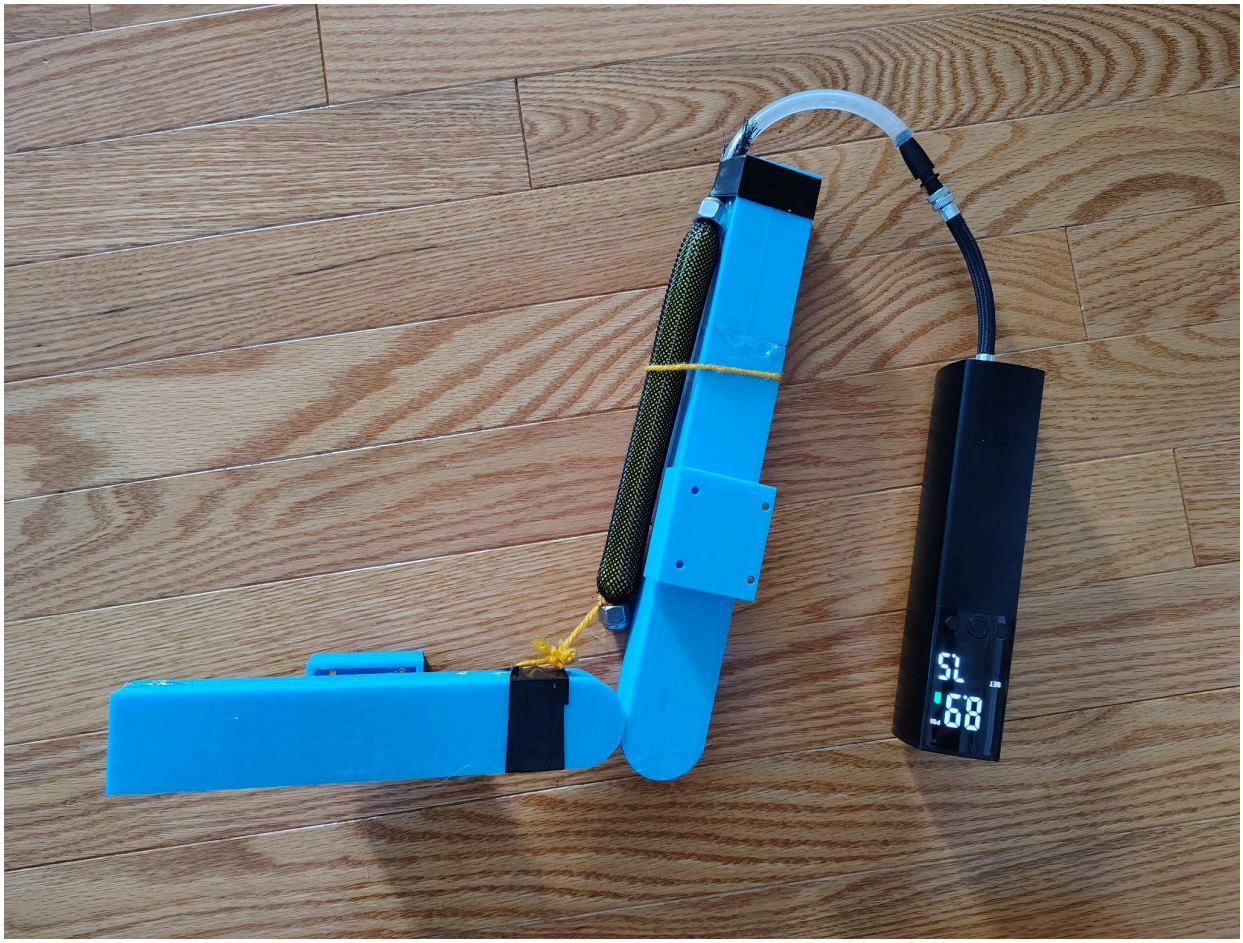
52
68

Section VI: References

Balakrishnan, H. (2025). *Whole new worlds: Multi-agent systems for advanced air mobility, aerial sensing, and more* [Lecture].

Cao, C. (2020). *Inherently elastic actuation for soft robotics* [Unpublished manuscript]. https://doi.org/10.13140/RG.2.2.30006.04166

Chiang, S. (2022). *Hybrid robotic manipulator using sensorized articulated segment joints with soft inflatable rubber bellows*. IEEE Xplore. https://ieeexplore.ieee.org/document/9724119

Furst, A. (2025, February 11). *Microbial engineering for human and environmental health* [Video]. YouTube. https://www.youtube.com/watch?v=njmRqLunlHI

Guo, Y., Liu, L., Liu, Y., & Leng, J. (2021). Review of dielectric elastomer actuators and their applications in soft robots. *Advanced Intelligent Systems, 3*(10), Article 2000282. https://doi.org/10.1002/aisy.202000282

Hajiesmaili, E., & Clarke, D. R. (2021). Dielectric elastomer actuators. *Journal of Applied Physics, 129*(15), Article 150902. https://doi.org/10.1063/5.0043959

Issue-integrated bionic knee restores versatile legged movement after amputation. (2023). *Nature Biomedical Engineering, 7*(5), 517–526. https://doi.org/10.1038/s41551-023-01087-z

Ji, X., Liu, X., Cacucciolo, V., Imboden, M., Civet, Y., El Haitami, A., Cantin, S., Perriard, Y., & Shea, H. (2019). An autonomous untethered fast soft robotic insect driven by low-voltage

dielectric elastomer actuators. *Science Robotics, 4*(37), Article eaaz6451. https://doi.org/10.1126/scirobotics.aaz6451

Kaneko, K., Kaminaga, H., Sakaguchi, T., Kajita, S., Morisawa, M., Kumagai, I., & Kanehiro, F. (2019). A robot HRP-5P: An electrically actuated humanoid robot with high-power and wide-range joints. *IEEE Robotics and Automation Letters, 4*(2), 1431–1438. https://doi.org/10.1109/LRA.2019.2896465

Knapp, M. (2025, January 21). *Exploring the last spectral frontier: The Great Observatory for Long Wavelengths (GO-LoW)* [Video]. YouTube. https://www.youtube.com/watch?v=ghDqLWbeQUA

Mao, G., Drack, M., Karami-Mosammam, M., Wirthl, D., Stockinger, T., Schwödiauer, R., & Kaltenbrunner, M. (2020). Soft electromagnetic actuators. *Science Advances, 6*(26), Article eabc0251. https://doi.org/10.1126/sciadv.abc0251

Newman, D. (2025, February 4). *Leading innovation: Exploring optimistic futures* [Video]. YouTube.

Onishi, N. (2025, January 14). *Update on Wind Challenger – Innovation of wind propulsion of ships: May the "Wind Force" be with you* [Video]. YouTube. https://www.youtube.com/watch?v=a-CEWnzc1Ys

PneuNets bending actuators. (n.d.). Soft Robotics Toolkit. https://softroboticstoolkit.com/book/pneunets-bending-actuator

Rothemund, P., Kellaris, N., Mitchell, S. K., Acome, E., & Keplinger, C. (2020). HASEL artificial muscles for a new generation of lifelike robots—Recent progress and future opportunities. *Advanced Materials, 33*(19), Article 2003375. https://doi.org/10.1002/adma.202003375

Xavier, M. S., Tawk, C. D., Zolfagharian, A., Pinskier, J., Howard, D., Young, T., Lai, J., Harrison, S. M., Yong, Y. K., Bodaghi, M., & Fleming, A. J. (2022). Soft pneumatic actuators: A review of design, fabrication, modeling, sensing, control and applications. *IEEE Access, 10*, 59442–59485. https://doi.org/10.1109/access.2022.3179589

Yong, X., Luo, X., Zhao, H., Qiao, C., Li, J., Yi, J., Yang, L., Oropeza, F. J., Hu, T. S., Xu, Q., & Zeng, H. (2022). Recent advances in biomimetic soft robotics: Fabrication approaches, driven strategies and applications. *Soft Matter, 18*(40), 7699–7734. https://doi.org/10.1039/d2sm01067d

Zaidi, S., Maselli, M., Laschi, C., & Cianchetti, M. (2021). Actuation technologies for soft robot grippers and manipulators: A review. *Current Robotics Reports, 2*(3), 355–369. https://doi.org/10.1007/s43154-021-00054-5